Vol. 40, No. 4 (2018) 624-632, DOI: 10.24874/ti.2018.40.04.09

Tribology in Industry

www.tribology.rs

RESEARCH

Tribocorrosion Behavior of Niobium-Based Thin Films for Biomedical Applications

P. Guzman[a], J.L. Caballero[a], G. Orozco-Hernández[b], W. Aperador[a], J.C. Caicedo[c]

[a]*School of Engineering, Universidad Militar Nueva Granada, Bogotá, Colombia,*
[b] *Faculty of Engineering, Universidad ECCI, Colombia,*
[c] *Tribology, Polymers, Powder Metallurgy and Processing of Solid Recycled Research Group, Universidad del Valle, Cali, Colombia.*

Keywords:

Niobium
Carbide
Nitride
Electrochemical and tribological properties

Corresponding author:

Willian Aperador
Universidad Militar Nueva Granada
Cra 11 # 101 -80, Bogotá-Colombia.
E-mail: g.ing.materiales@gmail.com

A B S T R A C T

The current work presents a comparative study of niobium, niobium carbide, and niobium nitride coatings deposited on AISI 316LVM stainless steel. The investigation was based on the synergy between corrosion and wear; therefore, the coating application was focused on future biomedical implants. The experiments were conducted under conditions of simulated biological fluid, with load and speed parameters of an average person. The tribo-corrosion tests were done by adapting an electrochemical cell to a pin-on-disk tribometer. The surfaces were characterized through optical means and scanning electron microscopy while the corrosion phenomenon was studied by potentiodynamic polarization curves. As a result, it was found that these coatings protect the surface against corrosion showing no evidence of degradation and lower corrosion rate value compared with the uncoated steel substrate. Moreover, the coatings show diverse wear mechanisms including abrasion wear and plastic deformation. The microstructure of the niobium coating was modified by the addition of carbon or nitrogen, improving the surface performance. Furthermore, in all the studied cases the coatings showed better behavior in tribo-corrosion phenomena in relation to the AISI 316LVM stainless steel substrate.

© 2018 Published by Faculty of Engineering

1. INTRODUCTION

Metallic materials and their compounds have been widely used in several fields comprising mechanical structures, ornamentation, electronic devices and medicine amongst others. Regarding medical applications, they play an important role in surgical devices, manufacturing of medical implants, as well as instrumentation. In addition, the biomedical materials must accomplish the requirement of biocompatibility due to their continuous contact with live tissues inside the body environment [1–4]. Implants and parts in general that are in contact with aggressive environments are subject to degradation phenomena creating a demand of properties like high values of physical resistance and excellent anticorrosive behavior. Corrosion and wear mechanisms generate a synergy that affects the integrity of the implant surface reducing its

lifetime [5–8]. Both phenomena together often induce several damages that can be extremely aggressive to the materials' surface and leads to the implant extirpation. The AISI 316LVM stainless steel can be defined as a versatile material due to its properties like ductility, elastic modulus, corrosion resistance, biocompatibility, and even an affordable low-cost material with superior attention in third world countries on medical solutions. However, in long-term implant solutions this material tends to degrade and alter the surrounding environment. To deal with the surface worsening, the application of hard coatings has been broadly applied. Techniques such as chemical vapor deposition (CVD) and physical vapor deposition (PVD) allow to apply a thin film of a huge variety of materials with different composition and microstructure [9,10]. It is well known that the microstructure determines properties such as hardness, fatigue strength, chemical stability, adherence and conductivity, amongst others [11]. So, materials of group V from the periodic table have been largely studied, transition metals as tantalum and niobium have been applied in the biomaterials field in recent years due to the properties they exhibit inside the human body [12–16]. Niobium has largely been used in titanium alloys because of its good corrosion resistance, osteogenesis and biocompatibility, in fact, it is one of the elements that does not produce adverse reaction with surrounding tissues [1,2,17,18]. In terms of mechanical properties Nb and its alloys have been used for their good mechanical resistance, high melting point and high hardness even as reinforcement particles on composite materials with metal matrix [19]. Taking into account the last discussion, the current paper focuses on the tribocorrosion effect of three protective coatings based on Nb, NbC and NbN grown over 316LVM intended for use as biomaterials. In this sense, this research is centered on the tribocorrosion study by using Ringer's lactate solution to simulate internal human body conditions. The degradation mechanism in each coating was examined and compared to the substrate, with the aim to find biomedical applications such as invasive implants.

2. Experimental Details

2.1 Coatings Deposition

The coatings were made by using a magnetron sputtering technique in an ATC-Orion 8 UHV unbalanced magnetron sputtering system. A four inche niobium target (99.99%) was used and powered in dc; power of 100 W in pure Ar with a pressure of 0.8 Pa at a substrate temperature of 300 °C and a deposition time of 180 minutes was needed to produce an average thickness of 2.8 μm. For the NbN films, power of 400 W, 0 V bias voltage, and gas mixture of 76 % Ar and 24 % N_2 was used at a working pressure of 0.6 Pa. The NbC coatings were deposited using a mix of Ar (99.999 %) and CH_4 (99.99 %) gases in discharging. The RF power applied to the Nb was 380 W and the direct current (DC) deposition temperature of 300 °C and 0 V bias voltage was used.

2.2 Coatings Characterizations

In order to identify the crystallographic phases of the different coatings an X-ray diffractometer was used (Panalytical model Empyrean). The configuration was a parallel plate collimator 0.27° with a classic scintillation detector. The parameters for the tests were a power of 40 kV with an intensity of 30 mA and sweep interval from 10° to 110°. The anode of the X-ray tube was from cobalt with Kα1 of 1.789 Å and Kα2 of 1.7928 Å with an incident ray radius of 240 mm. Counting time was 1.65 s with a step size of 0.0100 and omega of 0.5° for a total of 11010 points. Phase identification was carried out in HighScore Plus software (Version 4.1, Panalytical, Almelo, The Netherlands) with the ICSD and COD databases [20,21]. With the aim of studying the influence of the synergy between wear and corrosion, a tribocorrosion test was carried out using a MT60 NANOVEA Tribometer. To simulate the biological condition an animal-bone pin was used as the wear counterpart immersed in Ringer's lactate solution. The speed and load parameters were based on a gait pattern of an average person and were limited by the characteristics of the tribometer [22–24]. The test parameters selected are shown in Table 1 and the scheme of the test is shown in Fig. 1.

Table 1. Parameters used in the experiment.

Sliding pattern	Animal-bone pin
Pin diameter	4 mm
Normal load	3 N
Total length	50 m
Speed	4500 mm/min

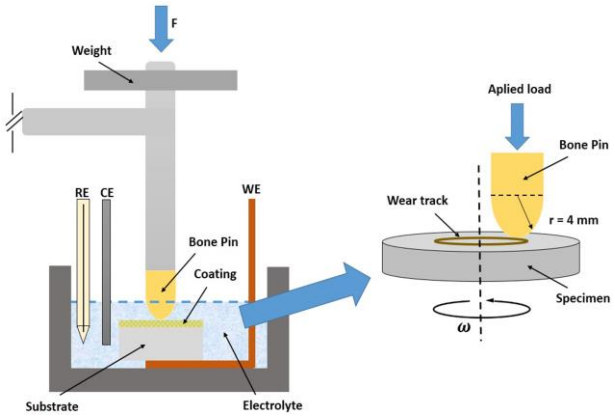

Fig. 1. Scheme of the tribometer test.

To obtain the friction coefficient the tribometer had software that controlled the equipment and also allowed to calculate this value. The tribometer was fitted with an electrochemical cell composed of a series of three electrodes, such as the reference electrode (Ag / AgCl), the counter-electrode (Platinum wire) and the workpiece located in a sample holder with a sample exposed area of 1 cm^2 and containing the electrolyte. A Gamry potentiostat - galvanostat model PCI-4 was used for the evaluation of the resistance to corrosion by using the potentiodynamic polarization technique. The measures were made with a scanning speed of 1 mV/s, in a voltage range from -250 mV to +250 mV with respect to corrosion potential (Ecorr), which was stabilized for 60 minutes. The corrosion velocity values (Vcorr) were calculated from the Tafel slopes method and the corrosion current density (Icorr) value in the potential range of ±250 mV vs. Ecorr, from the anodic polarization curves. Three replicate tests were performed for each group of specimens. Wear tracks and the surface damage generated by the bone pin were examined with a JEOL NeoScope JCM-5000 Scanning Electron Microscope to establish the wear nature. Wear tracks profiles were measured using a high-resolution optical microscope Leica DVM2500 model, which had a Leica Application Suite software for the analysis of 3D models.

3. RESULTS AND DISCUSSION

3.1 X-ray diffraction

Figure 2 shows the crystallographic phases presented for the three coatings. Nb spectrum shows reflections of the Nb_2 phase according to the COD reference pattern 96-411-1970 with peaks at 44.681°, 65.035°, 82.352° and 98.968° 2θ degrees with its respective crystallographic planes (011), (002), (112) and (022). NbC spectrum shows peaks corresponding to the phase Nb_1C_1 at 40.474°, 47.084°, 68.786° and 82.961° corresponding to crystallographic planes (111), (002), (022) and (113) respectively in accordance with ICSD 98-008-5810 reference pattern. In the samples of Nb and NbC the substrate is also presented as it can be seen in the peak of Fe_2 phase (COD - 96-901-3489) located at 51.101° and (011) as a crystallographic plane. Finally, the NbN sample diffractogram shows peaks of Nb_1N_1 phase according to the ICSD reference pattern 96-411-1970 with peaks at 41.352°, 48.121°, 70.421°, 85.079° and 89.847° representing crystallographic planes (111), (002), (022), (113) and (222) respectively.

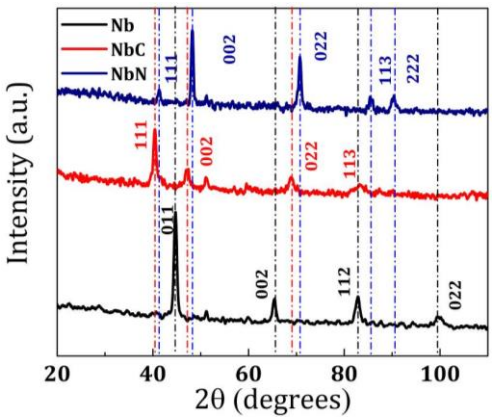

Fig. 2. XRD diagrams for the three materials Nb, NbC and NbN.

In all cases the cubic structure was predominant, however, Nb samples presented I m-3m spatial group while the other two coatings presented a Fm-3m spatial group. Niobium nitrides and carbides generate compounds with ionic and covalent bonds [25]; the ionic character for NbN is of 40.04 % and NbC presents an ionic character of 18.3 %. Introducing nitrogen or carbon atoms into the niobium crystalline structure induces structural changes from a body-centered cubic (BCC) with a cell parameter of 3.3280 Å to a NaCl like structure with a cell parameter of 4.4790 Å were Nb+ cations occupy interstitial sites between atomic sites of the FCC carbon cell [26].

3.2 Tribocorrosion Results

Figure 3 shows potentiodynamic polarization curves, from these results the anodic and cathodic

slopes values were found to use the Tafel method and then find the corrosion current density and its potential to calculate corrosion rate. This was done for the three samples and the uncoated substrate, immersed in Ringer's lactate solution while the pin-on-disk test was carried out simultaneously. From these results, it is observed that the NbC, NbN and Nb coatings deposited on the 316LVM substrates have corrosion current density values shifted to lower values compared to the uncoated substrate.

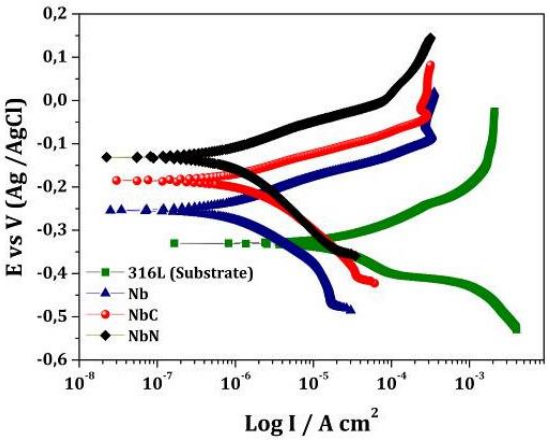

Fig. 3. Potentiodynamic polarization curves for AISI316LVM stainless steel substrate, as well as NbC, NbN and Nb coatings.

Table 2. Electrochemical values obtained from potentiodynamic polarization curves of each system.

	316LVM	Nb	NbC	NbN
Beta A / V/decade	81.30	76.20*10^{-3}	93.60*10^{-3}	85.30*10^{-3}
Beta C / V/decade	115. *10^{-3}	139.4*10^{-3}	166.0*10^{-3}	131.0*10^{-3}
Ecorr / mV	-138.0	-160.0	-153.0	-177.0
Icorr / µA	25.40	1.440	1.010	1.070
Corrosion Rate / mpy	58.36	3.314	2.325	2.462
Chi Squared	0.078	0.035	0.015	0.026

Moreover, Table 2 shows corrosion current densities and corrosion rate values for the three coatings and the substrate; from this it was found that metal nitrides and metal carbides exhibited better corrosion current density compared to the Nb coatings which exhibited higher corrosion rate values, and this is related to the evidenced deterioration attributed to the abrasive and adhesive wear processes. Nevertheless, the Nb coating improved the tribo-electrochemical performance in contrast with the substrate. Likewise, adding carbides and nitrides can result in a superior protection due to the fact that the corrosion current density was lower for both NbC and NbN systems [27]. However, the NbC coating showed an increased corrosion resistance compared with NbN, due to the fact that this coating has a higher percentage of covalent bonds, which means that more energy to break this interaction between Nb and C is necessary [28].

3.3 Coefficient of Friction

In the tribological test, the substrate was characterized to obtain its performance and then compare it with the coated samples. As can be seen in Fig. 4, the stainless-steel substrate showed an initial running-in process with the increasing coefficient of friction (Zone 1). This behaviour is associated to the surfaces in contact, in which the bone pin had a higher porosity entailing different contact points. The irregularities in the surfaces were gradually removed with the increase of the travel distance. Therefore, the contact area between the bodies, reduced the coefficient of friction and led the system to a friction transition in which it attempted to reach a steady-state (Zone 2) [29–33].

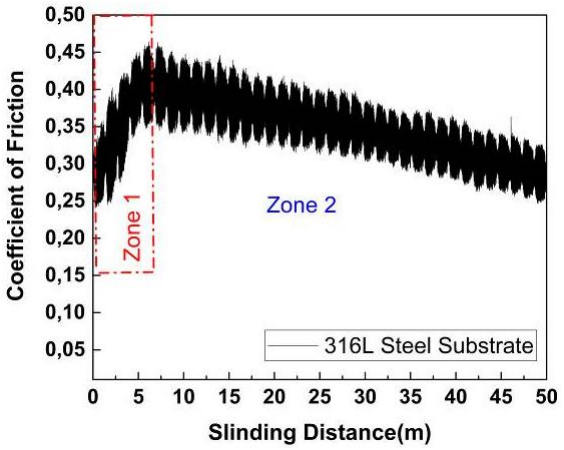

Fig. 4. Coefficient of Friction for AISI 316LVM stainless steel substrate.

Likewise, the behaviour of the coated samples exhibited the running-in curves, which are described by a constant friction with a final transition to a steady-state. Figure 5 shows the coefficient of friction results for all coatings (Nb, NbN, and NbC). So, the Nb coating exhibited the highest coefficient of friction values and this can be explained by three main factors; its microstructure, the interaction between the animal bone pin and the material surface, and the wear evidenced by SEM and optical microscope. Nonetheless, the coefficient of

friction value for the Nb coating was less compared with the value obtained for the uncoated substrate. In zone 1, the Nb coating tried to generate a layer that protected the surface against tribocorrosion, however, with the increase of the length traveled this layer tended to degrade and caused an increase in the coefficient of friction (zone 2). Finally, the behaviour tended to stabilize (steady-state), with low variations (zone 3).

On the other hand, the NbC and NbN coatings had a more stable behaviour related to the variation of the coefficient of friction range. So, these coatings showed a similar behaviour in zone 1, where the samples exhibited running-in curves, which were described by a constant increment of the coefficient of friction attributed to the surface homogenization and the rupture of the passive layer; however, in zone 2 with the increase of the travel distance, the protective film was worn off the surface. The coatings showed a stable behaviour and the lowest coefficient of friction value was for the NbC sample followed by the NbN sample [34,35]. Nitrides and carbides, as mentioned above, are substitutional in the Nb cubic structure; even when their properties are similar, the carbides have, for instance, less friction coefficient in comparison with nitrides [28,34].

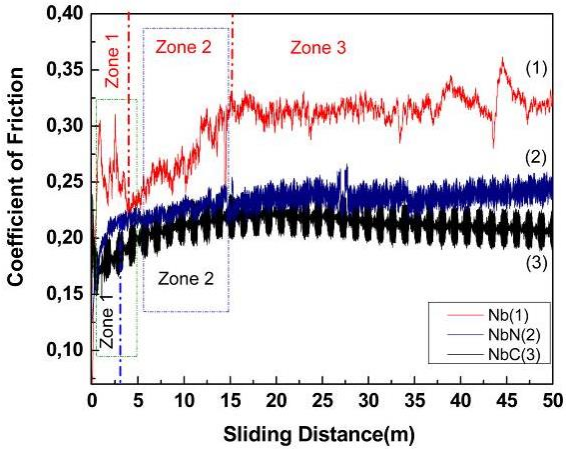

Fig. 5. Coefficient of Friction as a function of sliding distance for Nb, NbC and NbN coatings.

The coefficient of friction values that were obtained for all the coatings and the uncoated substrate are shown in Fig. 6. The high coefficient of friction value of the substrate can be related to the initial transient of the system as well as the irregularities of the surface. Also, the running-in curve behaviours are due to the high damage suffered by the surface and evidenced through the surface deterioration [36]. The surface modification introduced by the films, make the surfaces more homogeneous and stable on their contact with the animal bone pin; due to that the friction coefficients observed on all the coatings were reduced in relation to the uncoated substrate. This lead a transition to reach a steady-state in a shorter travelled distance compared to the uncoated 316LVM steel substrate.

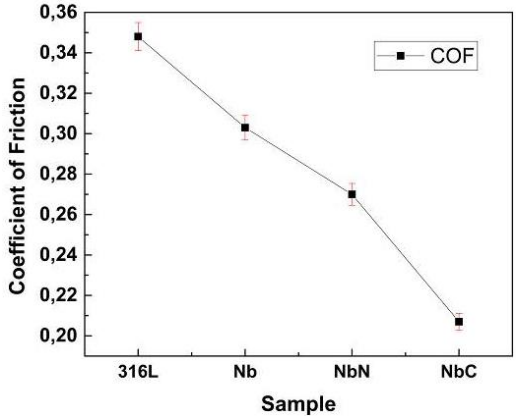

Fig. 6. Friction Coefficient for uncoated 316L steel substrate, Nb, NbN and NbC coatings.

3.4 SEM morphology

Coatings' surfaces were characterized by scanning electron microscopy (SEM) aiming to evidence the wear-corrosion phenomena. In the tribo-corrosion tests, the solution in contact with the coatings acted as a lubricant and consequently the adhesive wear was reduced. Likewise, abrasive wear was reduced when the friction between both materials was reduced due to the interface among them [37]. For the uncoated substrate, abrasive wear was identified due to the ploughing forming, as shown in Fig 7a. Moreover, in the sample coated with Nb, the adhesive wear was evidenced in zones where material was detached and some cracks appeared on the coating surface as can be seen in Fig. 7b. In addition, the formation of grooving and ploughing with material displacement towards the wear track edge was observed, showing a typical characteristic of abrasive wear. Additionally, the uncoated substrate exhibited high degradation caused by the corrosive phenomena that could have altered the substrate surface. On the other hand, the sample coated with NbN (Fig. 7c) exhibited lower abrasive wear compared to the uncoated substrate and Nb coatings, due to that the addition of nitrides tends to enhance mechanical and tribological properties [38,39].

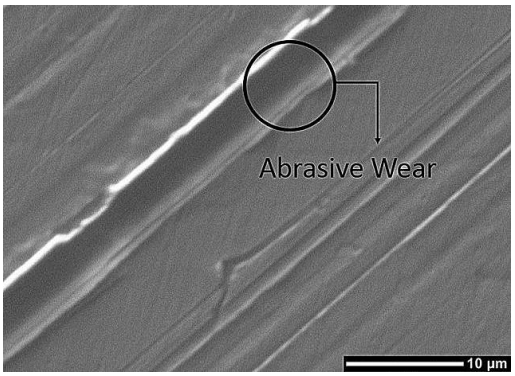

(a)

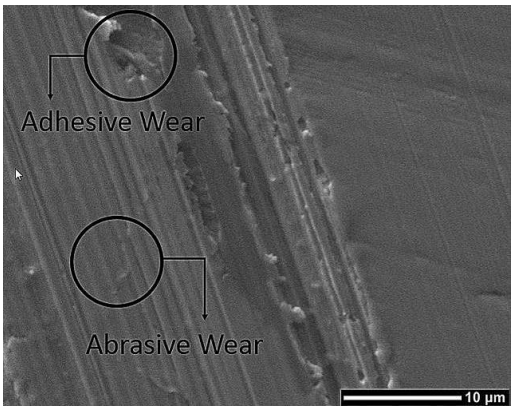

(b)

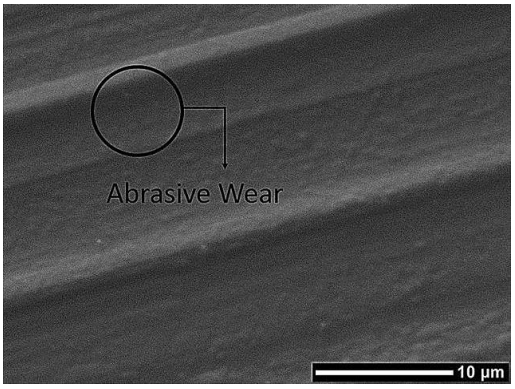

(c)

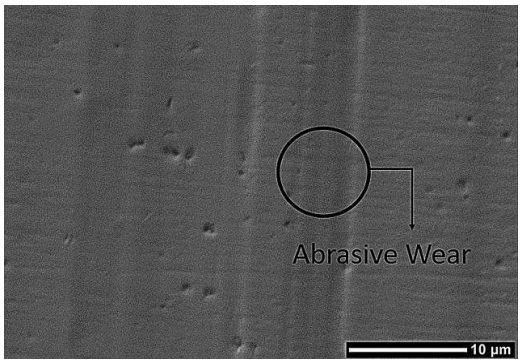

(d)

Fig. 7. SEM micrograph for all samples showing the wear track generated by pin-on-disk test: (a) wear track for uncoated 316L stainless steel substrate, (b) wear track for Nb coating, (c) wear track for NbN coating and (d) wear track for NbC coating.

However, in the micrograph of Fig. 7c a plastic deformation on the coating-substrate system is evidenced and could have been caused by many factors such as load and the solution surface interaction which acted as a lubricant making possible the abrasive wear reduction with ploughing formation and without cracks or the rupture presence associated to NbN coatings. Finally, the substrate coated with NbC exhibited the best behaviour in comparison with the rest of the samples, showing the lowest adhesive and abrasive wear mechanisms. Therefore, nitrides and carbides modify Nb structure generating thus a better cohesion between Nb-N and Nb-C atoms showing stronger bonds. Due to this, the surface hardness in the coatings increased and the adhesive and abrasive wear were diminished [40]. As can be seen in Fig. 7d the surface wear was the lowest in relation to the uncoated substrate, substrates coated with Nb and NbN systems.

3.5 Optical Microscope

After the tribo-corrosion tests, the wear tracks were measured to obtain the worn depth area (track height average) in all samples. In Fig. 8a the depth damage caused by the tribo-corrosion test on the uncoated substrate was observed; also, the track height value was around 4.62 µm and is related to the high change suffered by the surface. In the Nb sample the track height value was 3.40 µm, so this sample exhibited a advanced superficial deterioration as can be seen in Fig. 8b; a high value is related to morphological changes suffered like material removal attributed to the synergy between wear and corrosion. The substrate coated with NbN presented a track height of 1.85 µm, this value is related to the plastic deformation suffered by the nitride coating as can be seen in Fig. 8c, however, the variation on the surface coating (track height) was reduced in relation to the 316LVM substrate and Nb coatings. Finally, the NbC sample exhibited a track height of 0.130 µm being the lowest value of the coated samples (Fig. 8d), thus the high hardness and microstructure allowed a favourable response against wear-corrosion phenomena evidencing the least damage amongst all samples.

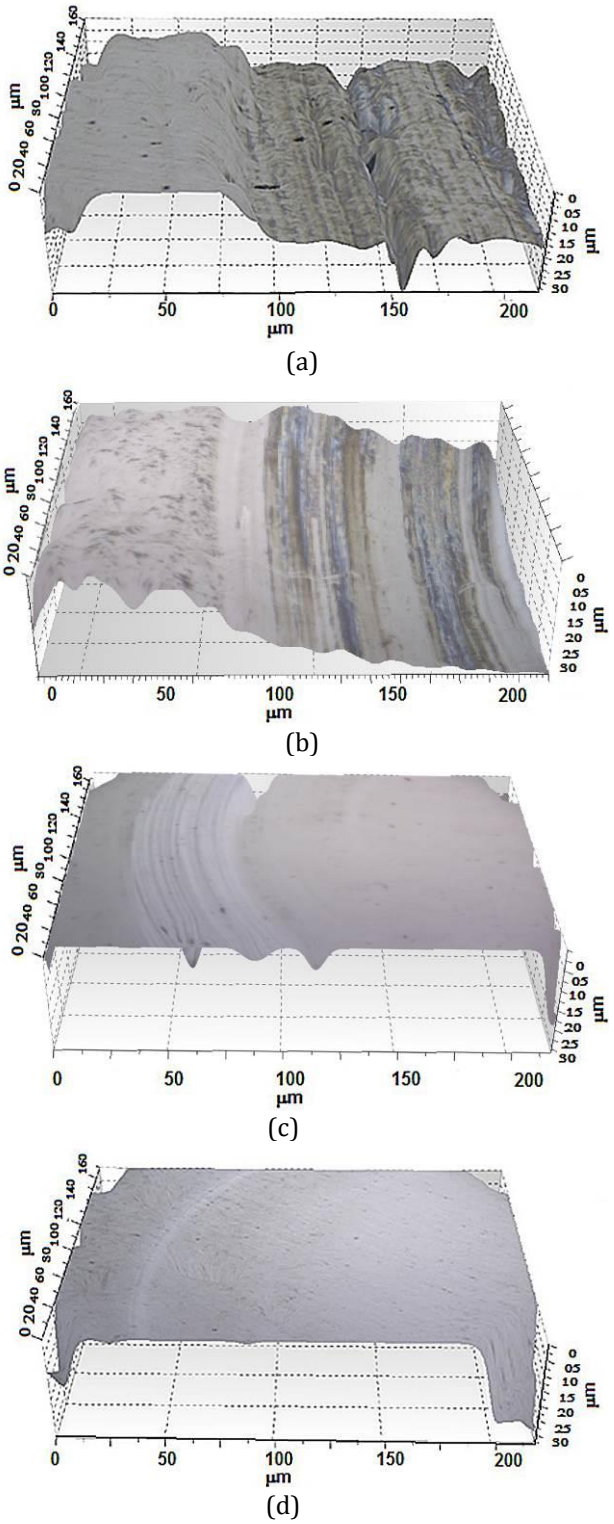

(a) (b) (c) (d)

Fig. 8. Optical profilometry showing the tribo-corrosion wear after the pin-on disk test obtained for all samples: (a) uncoated 316L stainless steel substrate, (b) Nb coatings, (c) NbN coatings and (d) NbC coatings.

Finally, correlating the tribo-electrochemical performance results with the experimental growth process, especially with the NbC system, it was observed that a microstructural modification of the system is achieved, showing that it is possible to find a surface with high density and high hardness. As can be seen in the profile image, the adhesion of the coatings had a slight variation in comparison with the Nb coating; the failure mode analysis permits to conclude that a fracture was presented by cracking related with the presence of the Nb_2 phase, and when this phase content decreased the wear was reduced. Therefore, the microstructure of the surface allows to appreciate that the NbN and NbC coatings exhibited better performance in relation to the uncoated substrate and the Nb coating; potentiodynamic curves showed a little passivation zone for the NbN and NbC coatings.

4. CONCLUSIONS

The aim of the present paper was to examine whether the different coatings could enhance the protection against the combined wear and corrosion phenomena compared with the uncoated substrate. Firstly, it was found that the coatings act as the sacrifice material function which suffers the damage avoiding substrate degradation. This evidence is highlighted in the lower corrosion value and lower friction coefficient obtained. Secondly, the coatings with addition of nitrogen and carbon have a superior performance related to the surface wear reduction and lower corrosion rate compared with uncoated 316L stainless steel substrate and substrate coated with Nb. This behaviour could be explained by the presence of Nb_1C_1 and Nb_1N_1 phases identified by means of XRD and the modification it induces in the Nb cubic structure. Finally, it was observed that the films can act as protective barriers, taking in account that the coatings were tested in tribo-corrosion conditions by using an animal bone pin as a counterpart.

Acknowledgement

This research was supported by" Vicerrectoría de investigaciones de la Universidad Militar Nueva Granada" under contract ING-2630-2018.

REFERENCES

[1] L.S. Saleh, S.J. Bryant, *In vitro and in vivo models for assessing the host response to biomaterials*, Drug

Discovery Today: Disease Models, vol. 24, pp. 13–21, 2017, doi: 10.1016/j.ddmod.2018.04.002

[2] J.J. Li, N. Sydney, L. Health, S. Leonards, *Tissue Response to Biomaterials*, Elsevier Inc., 2018.

[3] J. Liu, L. Chang, H. Liu, Y. Li, H. Yang, J. Ruan, *Microstructure, mechanical behavior and biocompatibility of powder metallurgy Nb-Ti-Ta alloys as biomedical material*, Materials Science & Engineering C, vol. 71, pp. 512–519, 2017, doi: 10.1016/j.msec.2016.10.043

[4] S.A. Pauline, N. Rajendran, *Corrosion behaviour and biocompatibility of nanoporous niobium incorporated titanium oxide coating for orthopaedic applications*, Ceramics International, vol. 43, no. 2, pp. 1731–1739, 2017, doi: 10.1016/j.ceramint.2016.08.207

[5] M. Hasegawa, H. Wakabayashi, A. Sudo, *A case of bone necrosis with pseudotumor following metal-on-metal total hip arthroplasty*, Arthroplasty Today, vol. 4, no. 3 pp. 291–294, 2018, doi: 10.1016/j.artd.2017.09.008

[6] T. Yanisarapan, P. Thunyakitpisal, P. *Chantarawaratit, Corrosion of metal orthodontic brackets and archwires caused by fluoride-containing products: Cytotoxicity, metal ion release and surface roughness,* Orthodontic Waves, vol. 77, no. 2, pp. 79–89, 2018, doi: 10.1016/j.odw.2018.02.001

[7] K. Fallahnezhad, R.H. Oskouei, H. Badnava, M. Taylor, *An adaptive finite element simulation of fretting wear damage at the head-neck taper junction of total hip replacement: The role of taper angle mismatch*, Journal of the Mechanical Behavior of Biomedical Materials, vol. 75, pp. 58–67, 2017, doi: 10.1016/j.jmbbm.2017.07.003

[8] T. Hanawa, *Metal ion release from metal implants*, Materials Science and Engineering C, vol. 24, no. 6–8, pp. 745–752, 2004, doi: 10.1016/j.msec.2004.08.018

[9] D. Mattox, *Handbook of Physical Vapor Deposition* (PVD), Elsevier, 2010.

[10] H. Pierson, *Fundamentals of Chemical Vapor Deposition*, Elsevier, 1999.

[11] H. Holleck, *Material selection for hard coatings*, Journal of Vacuum Science and Technology A, vol. 4, no. 6, pp. 2661–2669, 1986, doi: 10.1116/1.573700

[12] A. Nouri, C. Wen, *Surface Coating and Modification of Metallic Biomaterials*, Elsevier, 2015.

[13] X. Yu, L. Tan, H. Yang, K. Yang, *Surface characterization and preparation of Ta coating on Ti6Al4V alloy*, Journal of Alloys and Compounds, vol. 644, pp. 698–703, 2015, doi: 10.1016/j.jallcom.2015.04.207

[14] G. Ramírez, S. E. Rodil, H. Arzate, S. Muhl, J.J. Olaya, *Niobium based coatings for dental implants*, *Appied* Surface Science, vol. 257, no. 7, pp. 2555–2559, 2011, doi: 10.1016/j.apsusc.2010.10.021

[15] L. Kunčická, R. Kocich, T.C. Lowe, *Advances in metals and alloys for joint replacement*, Progress in Materials Science, vol. 88, pp. 232–280, 2017, doi: 10.1016/j.pmatsci.2017.04.002

[16] S.P. Wang, J. Xu, *TiZrNbTaMo high-entropy alloy designed for orthopedic implants: As-cast microstructure and mechanical properties*, Materials Science and Engineering C, vol. 73, pp. 80–89, 2017, doi: 10.1016/j.msec.2016.12.057

[17] A.E.A. Maya, D.R. Grana, A. Hazarabedian, G.A. Kokubu, M.I. Luppo, G. Vigna, *Zr-Ti-Nb porous alloys for biomedical application*, Materials Science and Engineering C, vol. 32, no. 2, pp. 321–329, 2012, doi: 10.1016/j.msec.2011.10.035

[18] M. Braic, V. Braic, M. Balaceanu, A. Vladescu, C.N. Zoita, I. Titorencu, V. Jing, *Preparation and characterization of biocompatible Nb-C coatings*, Thin Solid Films, vol. 519, no. 12, pp. 4064–4068, 2011, doi: 10.1016/j.tsf.2011.01.193

[19] M.K. Han, J.Y. Kim, M.J. Hwang, H.J. Song, Y.J. Park, *Effect of Nb on the microstructure, mechanical properties, corrosion behavior, and cytotoxicity of Ti-Nb alloys*, Materials, vol. 8, no. 9, pp. 5986–6003, 2015, doi: 10.3390/ma8095287

[20] S. Graulis, D. Chateigner, R.T. Downs, A.F.T. Yokochi, M. Quirós, L. Lutterotti, E. Manakova, J. Butkus, P. Moeck, A. Le Bail, *Crystallography Open Database - An open-access collection of crystal structures*, Journal of Applied Crystallography, vol. 42, no. 4, pp. 726–729, 2009, doi: 10.1107/S0021889809016690

[21] T. Degen, M. Sadki, E. Bron, U. König, G. Nénert, *The HighScore suite*, Powder Diffraction, vol. 29, no. S2, pp. S13–S18, 2014. doi: 10.1017/S0885715614000840

[22] J.H. Hollman, F.M. Kovash, J.J. Kubik, R.A. Linbo, *Age-related differences in spatiotemporal markers of gait stability during dual task walking*, Gait and Posture, vol. 26, no. 1, pp. 113–119, 2007, doi: 10.1016/j.gaitpost.2006.08.005

[23] M.W. Whittle, *Clinical gait analysis: A review*, Human Movement Science, vol. 15, no. 3, pp. 369–387, 1996, doi: 10.1016/0167-9457(96)00006-1

[24] F. Taddei, S. Martelli, G. Valente, A. Leardini, M.G. Benedetti, M. Manfrini, M. Viceconti, *Femoral loads during gait in a patient with massive skeletal reconstruction*, Clinical Biomechanics, vol. 27, no. 3, pp. 273–280, 2012, doi: 10.1016/j.clinbiomech.2011.09.006

[25] R.C. Evans, *An Introduction to Crystal Chemistry*, Cambridge University Press, Cambridge, p. 424, 1964.

[26] H.O. Pierson, *Carbides of Group IV*, in Handbook of Refractory Carbides and Nitrides, Elsevier, pp. 55–80, 1996

[27] Z. Han, X. Hu, J. Tian, G. Li, G. Mingyuan, *Magnetron sputtered NbN thin films and mechanical properties*, Surface and Coatings Technology, vol. 179, no. 2–3, pp. 188–192, 2004, doi: 10.1016/S0257-8972(03)00848-X

[28] G.E. Cavigliasso, M.J. Esplandiu, V.A. Macagno, I*nfluence of the forming electrolyte on the electrical properties of tantalum and niobium oxide films: an EIS comparative study*, Journal of Applied Electrochemistry, vol. 28, no. 11, pp. 1213–1219, 1998, doi: 10.1023/A:1003449917148

[29] P.J. Blau, *Friction Science and Technology: From Concepts to Applications, Second Edition*, CRC Press, 2008.

[30] P.J. Blau, *On the nature of running-in*, Tribology International, vol. 38, no. 11–12, pp. 1007–1012, 2005, doi: 10.1016/j.triboint.2005.07.020

[31] J. Vetter, R. Rochotzki, *Tribological behaviour and mechanical properties of physical-vapour-deposited hard coatings: TiNx, ZrNx, TiCx, TiCx/i-C*, Thin Solid Films, vol. 192, no. 2, pp. 253–261, 1990, doi: 10.1016/0040-6090(90)90070-T

[32] D.H. Buckley, *Surface effects in adhesion, friction, wear and lubrication*, New York: Elsevier Science, 2000.

[33] K. Holmberg, H. Ronkainen, A. Laukkanen, K. Wallin, *Friction and wear of coated surfaces - scales, modelling and simulation of tribomechanisms*, Surfaces and Coatings Technology, vol. 202, no. 4–7, pp. 1034–1049, 2007, doi: 10.1016/j.surfcoat.2007.07.105

[34] X. Cai, Y. Xu, *Microstructure, friction and wear of NbC coatings on a Fe substrate fabricated via an in situ reaction*, Surface and Coatings Technology, vol. 322, pp. 202–210, 2017, doi: 10.1016/j.surfcoat.2017.05.046

[35] S. Barzilai, A. Raveh, N. Frage, *Inter-diffusion of carbon into niobium coatings deposited on graphite*, Thin Solid Films, vol. 496, no. 2, pp. 450–456, 2006, doi: 10.1016/j.tsf.2005.09.106

[36] M. Fellah, O. Assala, M. Labaiz, L. Dekhil, I. Alain, *Comparative study on tribological behavior of Ti-6Al-7Nb and SS AISI 316L alloys, for total hip prosthesis*, TMS 2014: 143rd Annual Meeting and Exhibition, vol. 2014, pp. 237–246, 2014, doi: 10.1007/978-3-319-48237-8_32

[37] G.W. Stachowiak, *Summary for Policymakers*, in Climate Change 2013 - The Physical Science Basis, Intergovernmental Panel on Climate Change, 23 - 26 September, 2013, Stockholm, Sweden, pp. 1–30.

[38] H. Ljungcrantz, *Nanoindentation hardness, abrasive wear, and microstructure of TiN/NbN polycrystalline nanostructured multilayer films grown by reactive magnetron sputtering*, Journal of Vacuum Science and Technology A, vol. 16, no. 5, p. 3104, 1998, doi: 10.1116/1.581466

[39] K.S. Havey, J.S. Zabinski, S.D. Walck, *The chemistry, structure, and resulting wear properties of magnetron-sputtered NbN thin films*, Thin Solid Films, vol. 303, no. 1–2, pp. 238–245, 1997, doi: 10.1016/S0040-6090(96)09529-6

[40] J.-E. Sundgren, H.T.G. Hentzell, *A review of the present state of art in hard coatings grown from the vapor phase*, Journal of Vacuum Science and Technology A, vol. 4, no. 5, pp. 2259–2279, 1986, doi: 10.1116/1.574062